Effect of pH on Complex Coacervate Core Micelles from Fe(III)−Based Coordination Polymer

ARTICLE *in* LANGMUIR · DECEMBER 2011

Impact Factor: 4.46 · DOI: 10.1021/la203449c · Source: PubMed

Langmuir

ARTICLE

pubs.acs.org/Langmuir

Effect of pH on Complex Coacervate Core Micelles from Fe(III)-Based Coordination Polymer

Junyou Wang,*,† Arie de Keizer,† Herman P. van Leeuwen,† Yun Yan,*,‡ Frank Vergeldt,§ Henk van As,§ Paul H. H. Bomans,∥ Nico A. J. M. Sommerdijk,∥ Martien A. Cohen Stuart,† and Jasper van der Gucht†

†Laboratory of Physical Chemistry and Colloid Science, Wageningen University, Dreijenplein 6, 6703 HB Wageningen, The Netherlands

‡Beijing National Laboratory for Molecular Sciences, State Key Laboratory for Structural Chemistry of Unstable and Stable Species, College of Chemistry and Molecular Engineering, Peking University, Beijing 100871, China

§Laboratory of Biophysics and Wageningen NMR Centre, Wageningen University, Dreijenplein 3, 6703 HA Wageningen, The Netherlands

∥Laboratory of Materials and Interface Chemistry and Soft Matter CryoTEM Research Unit, Department of Chemical Engineering and Chemistry, Eindhoven University of Technology, P.O. Box 513, 5600MB, Eindhoven, The Netherlands

ABSTRACT: The effect of pH on iron-containing complex coacervate core micelles [Fe(III)−C3Ms] is investigated in this paper. The Fe(III)−C3Ms are formed by mixing cationic poly(*N*-methyl-2-vinylpyridinium iodide)-*b*-poly(ethylene oxide) [P2MVP$_{41}$-*b*-PEO$_{205}$] and anionic iron coordination polymers [Fe(III)−L$_2$EO$_4$] at stoichiometric charge ratio. Light scattering and Cryo-TEM have been performed to study the variations of hydrodynamic radius and core structure with changing pH. The hydrodynamic radius of Fe(III)−C3Ms is determined mainly by the corona and does not change very much in a broad pH range. However, Cryo-TEM pictures and magnetic relaxation measurements indicate that the structure of the micellar cores changes upon changing the pH, with a more crystalline, elongated shape and lower relaxivity at high pH. We attribute this to the formation of mixed iron complexes in the core, involving both the bis-ligand and hydroxide ions. These complexes are stabilized toward precipitation by the diblock copolymer.

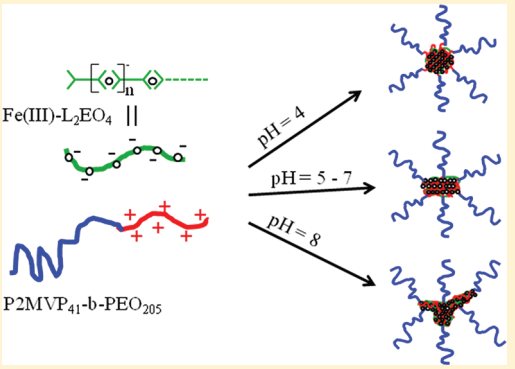

INTRODUCTION

Complex coacervate core micelles (C3Ms) are novel nanostructures formed by the electrostatically driven assembly of oppositely charged components. Such micelles are also called "polyion complex micelles" (PIC micelles)[1] or "block ionomer complex micelles" (BICs).[2] One of the components must be a polyion−neutral diblock copolymer, ensuring a neutral corona to stabilize the coacervate core. The other component could be an oppositely charged homopolymer,[3,4] another polyion−neutral diblock copolymer,[5,6] or a reversible coordination polymer.[7] The latter has a backbone consisting of metal ions coordinated by ditopic ligands [L$_2$EO$_4$] which can form C3Ms with metal ions in the core. Our group has recently investigated C3Ms with Zn^{2+}, Nd^{3+}, Fe^{2+}, and Fe^{3+} in the core.[8,9] The chemical structure of the polymer and the bis-ligand are shown in Scheme 1. Depending on the charge of the metal ions, each coordination center in the polymer carries a net −2 or −1 elementary charge. These negatively charged coordination polymers show a distribution that responds to changes in concentration or temperature. At low concentration and at a 1:1 metal to L$_2$EO$_4$ ratio, small rings consisting of only two monomers are predominant in solution.[10] Interestingly, these oligomers could still form C3Ms in the presence of oppositely charged diblock copolymers, indicating that confinement in the micellar core leads to a strong growth of the coordination polymers. C3Ms could only be formed in the presence of all three components (L$_2$EO$_4$, metal ions, and oppositely charged diblock copolymers); no C3Ms were formed in the absence of metal ions.[7]

Iron containing C3Ms (Fe−C3Ms) were studied in our previous work.[9] Such micelles are of interest, because the paramagnetic properties of the iron nuclei could make them suitable for MRI contrast agents, as an alternative for iron oxide particles. From the application point of view, stability is a very crucial aspect of C3Ms. C3Ms from covalent polyelectrolytes are sensitive to ionic strength and dissociate completely above a critical salt concentration (csc); in the case of weak polyelectrolytes, the structure and size also depend on the pH.[11−15] For metal-containing C3Ms, we have found that they were formed efficiently near charge stoichiometry and were very stable over time. An increase in salt concentration resulted in an increase of the cmc, a decrease in aggregation number, and swelling of the micelles followed by full dissociation at the csc.[9,16] However, the

Received: September 2, 2011
Revised: September 30, 2011
Published: October 28, 2011

Scheme 1. Structure of (a) P2MVP$_{41}$−PEO$_{205}$ and (b) L$_2$EO$_4$ and (c) Linear Structure of Coordination Complex Fe(III)−L$_2$EO$_4$

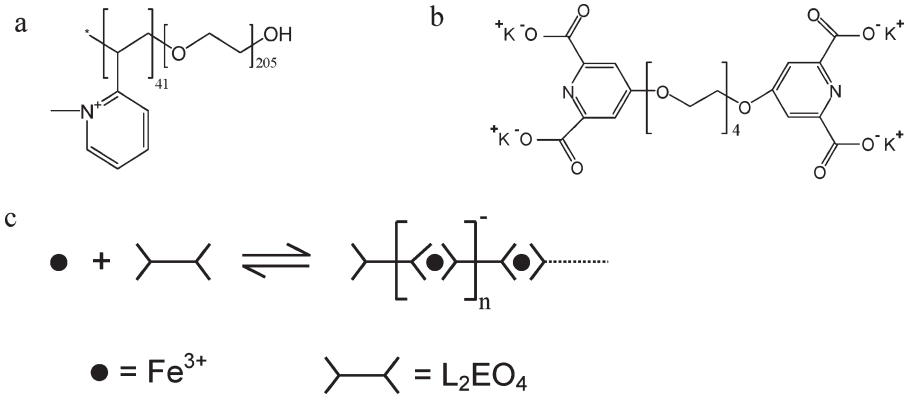

effect of pH on this kind of micelles has not been investigated. Since the diblock copolymer P2MVP$_{41}$-*b*-PEO$_{205}$ does not respond to pH, the pH response of the C3Ms is determined completely by the variation of coordination complexes with changing pH. At low pH, the ligand becomes protonated, destabilizing the coordination polymer. In the case of iron(III) as metal ion, hydroxide complexes can be formed at high pH, and these may be expected to affect the micellar structure and stability. In this paper, we focus on the effect of pH on Fe(III)−C3Ms.

EXPERIMENTAL SECTION

Materials. The diblock copolymer poly(*N*-methyl-2-vinylpyridinium iodide)-*b*-poly(ethylene oxide) (P2MVP$_{41}$-*b*-PEO$_{205}$) was obtained by quaternization of poly(2-vinylpyridine)-*b*-poly(ethylene oxide) (P2VP$_{41}$-*b*-PEO$_{205}$) (Polymer Source, M_w/M_n = 1.03, M_w = 13.3 k) following a procedure described elsewhere.[17] The degree of quaternization is about 90%. The bis-ligand compound 1,11-bis(2,6-dicarboxypyridin-4-yloxy)-3,6,9-trioxaundecane (L$_2$EO$_4$) was prepared according to the literature.[18] Iron chloride ($FeCl_3 \cdot 6H_2O$, analytical grade) and sodium nitrate ($NaNO_3$, analytical grade) were purchased from Aldrich and used without further purification. Fe(III)−L$_2$EO$_4$ coordination polymers were prepared by mixing solutions of $FeCl_3 \cdot 6H_2O$ and L$_2$EO$_4$ at a molar ratio of 1:1. The coordination center has one negative charge, as illustrated in Scheme 1. All samples were prepared in water with 10 mM NaCl; HCl and NaOH were used to adjust the solution pH.

Methods. *Light Scattering.* Light scattering at an angle of 90° was performed with an ALV light scattering-apparatus, equipped with a 400 mW argon ion laser operating at a wavelength of 514.5 nm. All the measurements were performed at room temperature.

The light scattering intensity is expressed as the excess Rayleigh ratio R_θ divided by the total polymer concentration. R_θ is obtained as

$$R_\theta = \frac{I - I_0}{I_{\text{toluene}}} R_{\text{toluene}} \quad (1)$$

where I is the scattering intensity of the micellar solution and I_0 is the intensity of the solvent. I_{toluene} is the scattering intensity of toluene, and R_{toluene} is the known Rayleigh ratio of toluene (2.4×10^{-2} m^{-1}). The total polymer concentration is the sum of the concentrations of all components contributing to micelles formation. The CUMULANT method was used to analyze the mean apparent hydrodynamic radius (R_h), which is

$$R_h = kTq^2/6\pi\eta\Gamma \quad (2)$$

where q is the scattering vector (~0.023 nm^{-1} at 90°), k is the Boltzmann constant, T is the absolute temperature, η is the viscosity of the solvent, and Γ is the measured average decay rate of the correlation function. The CONTIN method is used to analyze the distribution of particle (C3Ms) radii.

Cryogenic Transmission Electronic Microscopy (Cryo-TEM). The TEM grids were surface plasma treated using a Cressington 208 carbon coater operating at 5 mA for 40 s prior to the sample preparation. A few microliters of sample were placed on a TEM grid and the excess of liquid was removed with filter paper, followed by shooting the grid into liquid ethane cooled to −170 °C. The sample vitrification procedure was carried out using an automated vitrification robot (FEI Vitrobot Mark III) equipped with a humidity and temperature chamber. Samples were studied on a CryoTitan microscope (FEI) equipped with a field emission gun (FEG) operating at 300 kV and a postcolumn Gatan Energy Filter (GIF). Images were recorded using a post-GIF 2K × 2K Gatan CCD camera. For each sample, images were collected for a number of different regions in the sample.

NMR Relaxation Time Measurement. The longitudinal relaxation times T_1 of aqueous solutions of Fe(III)−C3Ms were measured using a Maran Ultra spectrometer (Resonance Instruments, Abingdon, UK) operating at 30.9 MHz proton resonance frequency. A combined inversion recovery Carr−Purcell−Meiboom−Gill (IR-CPMG) pulse sequence was used to measure T_1. Data were analyzed using a home-written IDL program (Research Systems Inc., Boulder, CO) and expressed as the relaxivity $r_1 = [(1/T_1) - (1/T_{1,0})]/C_{\text{Fe(III)}}$, with $T_{1,0}$ being the relaxation time in pure water.

RESULTS AND DISCUSSION

Effect of pH on Coordination Complex Fe(III)−L$_2$EO$_4$. Before discussing the effect of pH on the Fe−C3Ms, we first consider the pH dependence of the iron coordination polymer in the absence of the diblock copolymer. The stability of the coordination polymer is determined by the strength of the FeL_2^- complexes (iron ion bound to two ligand groups), as these complexes form the backbone of the coordination polymer (see Scheme 1c).

The speciation of Fe^{3+} is rather complex and involves, besides the FeL^+ (iron ion bound to one ligand group) and FeL_2^- species, also various hydroxide complexes and mineral phases, depending on the pH. Here we discuss the distribution of the various species in solutions of Fe^{3+} and L$_2$EO$_4$ by combining UV/vis spectroscopy and equilibrium speciation calculations. Only the FeL^+, FeL_2^-, and soluble iron hydroxide species are taken into account. All the equilibrium constants are available in the literature:[19,20] log $K_{a1(HL)}$ = 2.1, log $K_{a2(HL)}$ = 4.383; log $\beta_{(FeL)}$ = 10.91,

dx.doi.org/10.1021/la203449c |*Langmuir* 2011, 27, 14776–14782

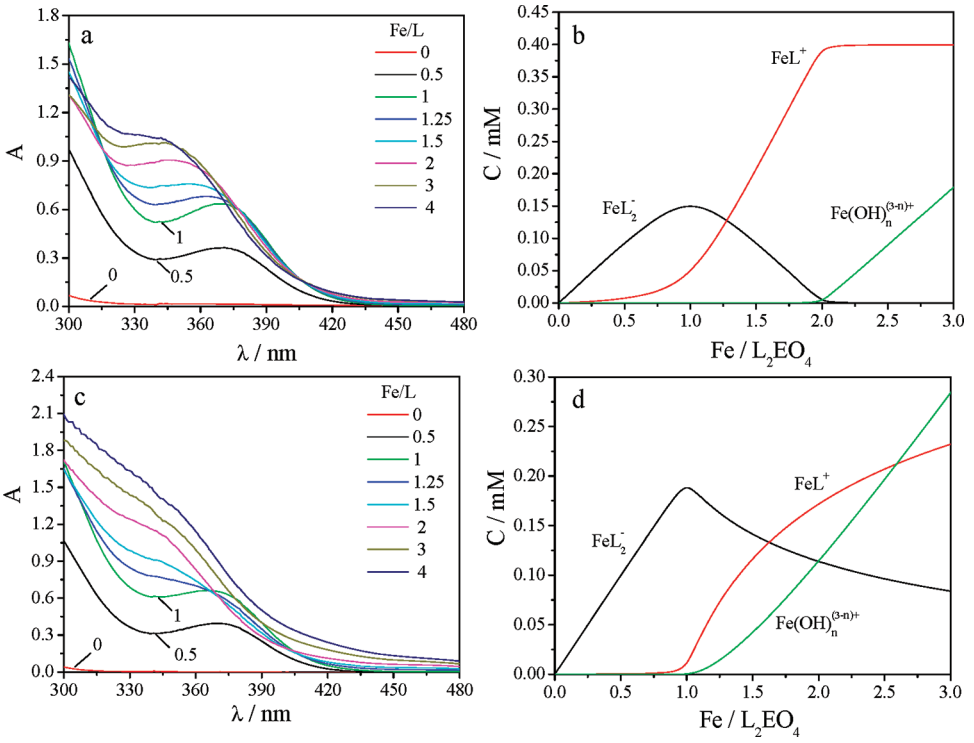

Figure 1. UV−vis spectra of titration of L_2EO_4 (0.2 mM) solution with Fe^{3+} for different metal to ligand ratios at pH 3 (a) and pH 5 (c). Calculated equilibrium speciation as a function of Fe/L ratio at pH 3 (b) and pH 5 (d). Values for the various equilibrium constants, obtained from literature, are reported in the text. FeL^+ and FeL_2^- represent the complexes with iron ion bounding to one and two ligand groups respectively and $Fe(OH)_n^{(3-n)+}$ is the sum of all soluble iron hydroxides [$Fe(OH)^{2+}$, $Fe(OH)_2^+$, $Fe(OH)_3$, and $Fe(OH)_4^{-1}$].

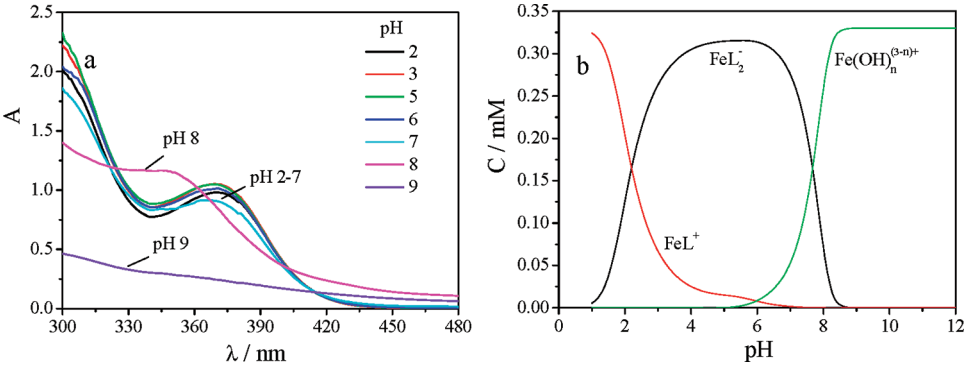

Figure 2. UV−vis spectra of Fe(III)−L_2EO_4 (1:1) complexes (a) and calculated curve of equilibrium speciation at different pH (b).

$\log \beta_{(FeL2)} = 17.13$; $Fe(OH)_n^{(3-n)+}(aq)$: $\log \beta_{11} = 11.81$, $\log \beta_{12} = 22.31$, $\log \beta_{13} = 28.91$, $\log \beta_{14} = 34.4$.

In Figure 1a, we show absorbance spectra for solutions at different Fe/L_2EO_4 ratios at pH 3, where iron hydroxide complexes are insignificant. In Figure 1b, we show the expected equilibrium distribution as a function of the metal to ligand ratio calculated using the equilibrium constant listed in the text above. When the ligand is in excess, an absorbance peak is observed around 370 nm. This peak can be attributed to FeL_2^- complexes that form predominantly under these conditions.[21,22] Under excess metal conditions, the peak gradually disappears, while a new peak appears around 350 nm, which is ascribed to the formation of FeL^+ complexes, as can be seen from Figure 1b. We conclude from this that the absorbance peak at 370 nm can be used to identify the presence of FeL_2^- complexes.

Figure 1c,d shows the absorbance spectra and calculated species distributions for various Fe/L_2EO_4 ratios at pH 5. Under excess ligand conditions, FeL_2^- is still the dominant species, as indicated by the absorbance peak. However, in the excess metal regime this peak disappears more rapidly than at pH 3. The speciation diagram suggests that this is related to the formation of iron hydroxide complexes.

Figure 2a shows absorbance spectra at a 1:1 Fe/L_2EO_4 ratio for different pH and Figure 2b shows the corresponding species distributions obtained from the equilibrium calculation. FeL^+ is dominant in solution when pH <2, because part of the ligand groups are protonated at low pH, making them less available for complexation with iron. Above this pH, anionic 1:2 complexes FeL_2^- become the main complexes in solution. Upon further increasing the pH, more and more iron hydroxide complexes form,

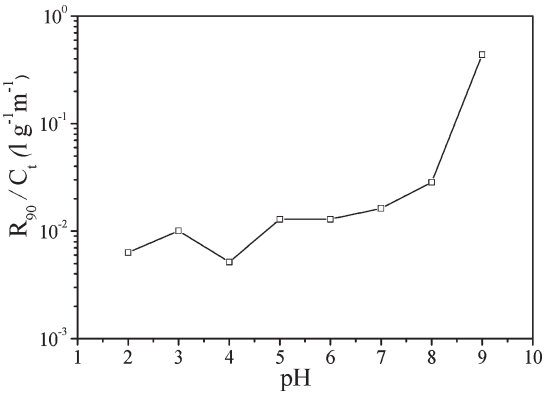

Figure 3. Light scattering intensity of Fe(III)−L_2EO_4 coordination complexes without diblock copolymer at different pH.

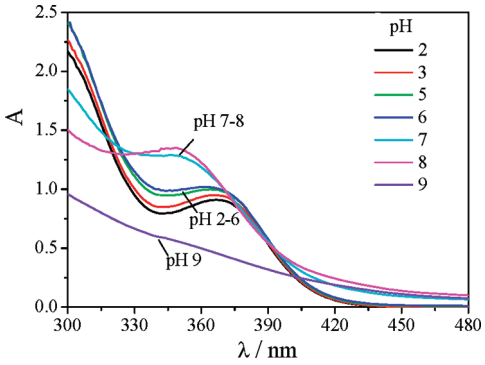

Figure 4. UV−vis spectra of Fe(III)−C3Ms at different pH values.

leading to dissociation of the coordination polymer. Indeed, the absorbance peak decreases between pH 6 and 7 and disappears near pH 8. A peak around 350 nm appears at pH 8. However, it cannot be due to FeL^+ complexes, because their concentration is very low at this high pH (Figure 2b). We suppose that it is due to mixed FeLOH complexes, which are not taken into account in the calculations. We can conclude from this that FeL_2^- complexes are the dominant species between pH 2 and 7. Coordination polymers should therefore be stable at 1:1 Fe/L_2EO_4 ratio in this pH range.

Bombi et al.[20] have studied iron coordination complexes with the monoligand (L) and found a brown precipitate at pH above 5 (depending on metal and ligand concentrations). They attributed this to the formation of insoluble $Fe(OH)_3$. In our system, a brown precipite can be found above pH 6 only at high ionic strength (1 M NaCl). At lower ionic strength (10 Mm NaCl), the solution of Fe(III)−L_2EO_4 is transparent until pH 9. However, light scattering performed at different pH values clearly shows that aggregates are formed at pH >7, as can be seen from an increase in light scattering intensity at low ionic strength (Figure 3). These aggregates are probably stabilized against further association by a surface charge leading to repulsion. At pH 9, precipitation occurs already at low ionic strength, and the scattering intensity increases strongly. In order to characterize the precipitation that was observed after adding salt, we collected the precipitate formed at pH 6 (1 M NaCl) and redispersed it in water by decreasing the salt concentration. When measuring the absorbance spectrum, we found the characteristic peak at 370 nm, indicating that the precipitate in our system contains FeL_2^- complexes and is not just $Fe(OH)_3$, as found by Bombi et al. for iron in the presence of the monoligand. We presume that the precipitate contains a mixture of iron complexes involving both ligand groups and hydroxide ions. Mixed complexes, such as FeLOH have indeed been reported.[20] At pH > 8, where the characteristic absorption peak has disappeared, the precipitate is probably dominated by $Fe(OH)_3$. To confirm this, we redissolved the precipitate formed at pH 9 by adding HCl. The resulting solution did not show the absorbance around 370 nm in the UV/vis spectrum, showing that there was indeed no ligand in the precipitate.

Effect of pH on Fe(III)−C3Ms. We have seen that iron hydroxide formation leads to disruption of the coordination polymers at pH >8. Now we investigate what happens if the coordination polymer is confined to the core of a C3M. The formation of Fe(III)−C3Ms has been studied in detail in our previous work.[9] Micelles in this study are prepared following the same strategy, by mixing cationic−neutral diblock copolymers $P2MVP_{41}$-*b*-PEO_{205} and anionic iron coordination polymers Fe(III)−L_2EO_4 at stoichiometric charge ratio.

To see whether the micellization induced by the diblock copolymer has an effect on the speciation, we show in Figure 4 absorbance spectra of Fe(III)−C3Ms at different pH values. The characteristic absorption peak for the FeL_2^- complexes can be seen at low pH. However, compared to coordination complexes without diblock copolymer (Figure 2a), the absorbance peak disappears already at pH 7 instead of 8. This means that confinement of the coordination polymer in the core of a micelle facilitates hydroxide formation. This could be due to a locally higher concentration of FeL_2^- complexes in the core. Additionally, the cationic block of the copolymer could locally create a positively charged domain, where the pH is higher than that in the bulk solution. This would cause the disruption of the coordination polymer already at lower bulk pH.

Figure 5 shows the light scattering data of Fe(III)−C3Ms as a function of pH. Both the light scattering intensity and the hydrodynamic radius obtained from the cumulant analysis do not change very much from pH 2 to 8. Larger aggregates form at pH 9, leading to an increase of the light scattering intensity. However, these aggregates are still stable structures. We did not find any brown precipitate, even after several weeks in the micellar solution. Hence, the block copolymer stabilizes the iron complexes against continued aggregation. When either the block copolymer or the ligand are left out, a brown precipitation was observed after several hours at pH 9, which means that the ligand and diblock copolymer are both needed to stabilize the structures. CONTIN analysis in Figure 3b confirms the result from cumulant analysis. The micellar size and size distribution do not change very much from pH 2 to 8. The peak at pH 9 shifts to a bigger size and a broader distribution.

pH-Dependent Core Structure of Fe(III)−C3Ms. Cryo-TEM pictures in Figure 6 show the micellar core structure at different pH values. A striped core structure is observed with different shapes in a broad pH range (4−8). A similar structure has been found in previous work.[21] At pH 4, the stripes in the core have a length of 20−30 nm and a space between them of 1−2 nm. This spacing is comparable to the size of the Fe(III)−L_2EO_4 complex, which is the dominant coordination complex in the system at this pH, as shown above. We therefore believe that the stripes are formed by aligned coordination polymers, probably associated with the cationic blocks of the diblock copolymer (Scheme 2). The neutral corona from the copolymer stops continuous growth

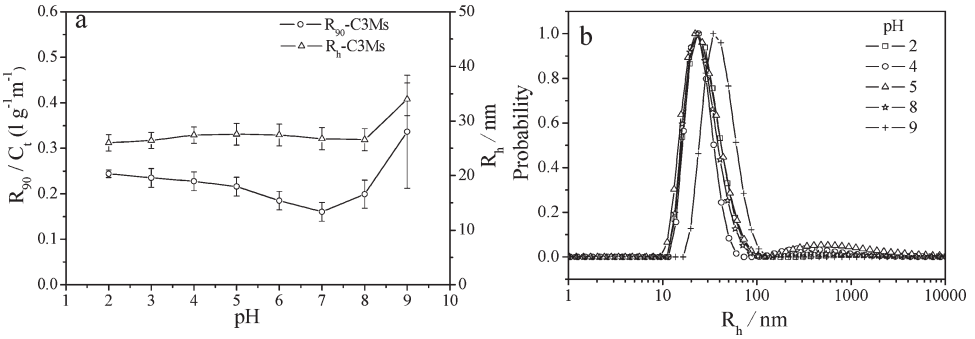

Figure 5. (a) Variations of light scattering intensity and hydrodynamic radius at different pH. (b) CONTIN analysis of particle size and size distribution (Γ weighted) at different pH values.

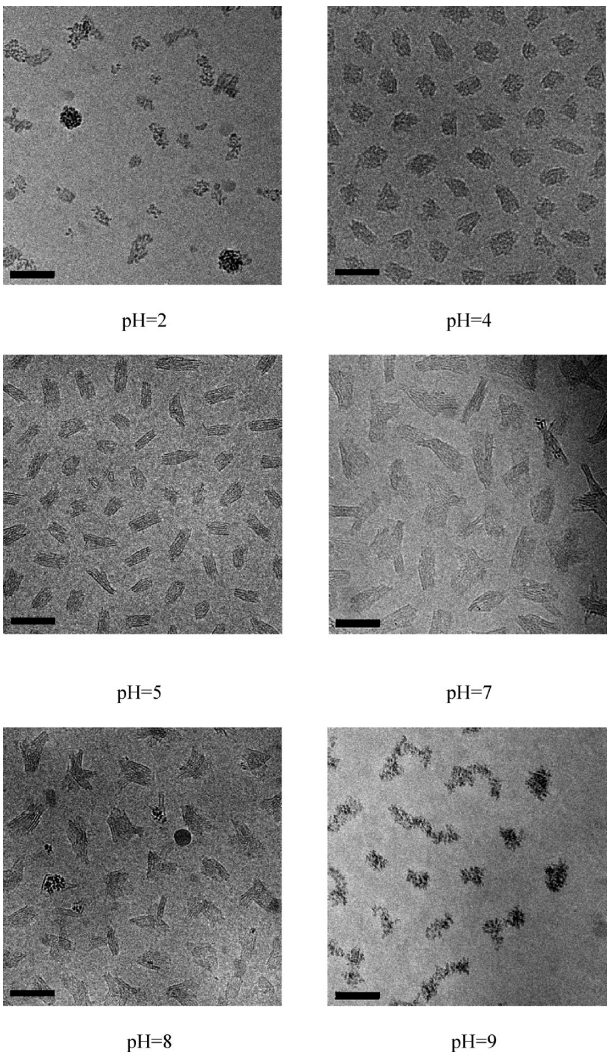

Figure 6. Cryo-TEM pictures of Fe(III)−C3Ms at different pH values; every bar represents 50 nm.

and irregular aggregation, leading to monodispersed spherical particles. We note that rodlike coordination polymers were observed recently by Kurth et al.[23,24] for solutions containing iron and a rigid bis-ligand, 1,4-bis(2,2′:6′,2″-terpyridin-4′-yl)-benzene. In our system, the Fe(III)−L_2EO_4 complexes do not form rod-like structures in solution due to the flexible EO-linker

Scheme 2. Illustration of the Formation of the Striped Core Structure of Fe(III)−C3Ms

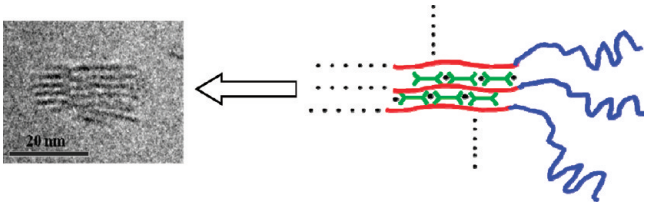

between the ligand groups. Probably, the diblock copolymer assists by aligning the Fe(III)−L_2EO_4 coordination polymer along the charged block by electrostatic coacervation.

Rodlike structures have also been observed for iron hydroxide in the presence of a polymer network.[25,26] However, the absorbance spectra discussed above (Figure 2) show that at pH 4 the coordination polymer is the dominant species in the system, while there is very little iron hydroxide. Nevertheless, hydroxide ions probably do play a role, since similar structures were never observed with less acidic metal ions, such as Zn^{2+} and Nd^{3+}. Moreover, changing the pH clearly has an effect on the shape of the micellar cores. At low pH (pH 2), where hydroxide ions do not play a role, the regular striped structure in the core is absent and instead irregular aggregates are formed that contain small dark particles. Protonation of the ligands, leading to weakening of the electrostatic interaction, may also disrupt the core structure at low pH. Above pH 4, the striped structures are formed and at higher pH these structures become more asymmetric. The width of the stripe does not change but the length goes up to 25−40 nm upon changing the pH from 5 to 7, leading to an elongated core shape. At pH 7, some branched or starlike shapes appear in solution, which are more numerous at pH 8. The high concentration of hydroxide ions at this pH may induce a multidirectional growth of iron complexes, leading to these special structures. At pH 9, more irregular particles are observed containing small dots, similar to the structures observed at pH 2. From the absorbance spectra, however, we can see that these particles must be very different from the particles observed at pH 9. At this high pH, the coordination polymer is disrupted, so that these particles are probably iron hydroxide particles that are stabilized against precipitation by the diblock copolymer.

Although the structure of the core was observed to change between pH 2 and 8 by UV/vis spectroscopy and cryo-TEM images, light scattering did not show any significant changes.

dx.doi.org/10.1021/la203449c |*Langmuir* 2011, 27, 14776–14782

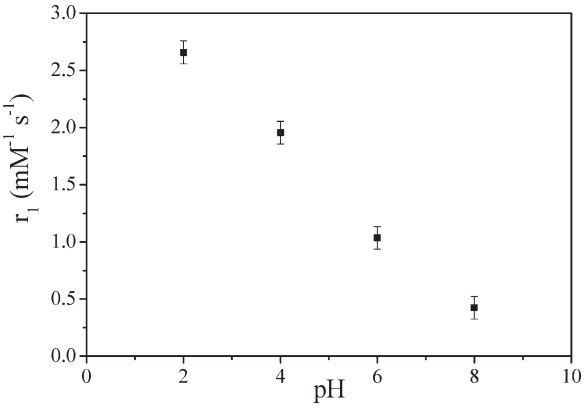

Figure 7. Effect of pH on the relaxivity r_1 of Fe(III)−C3Ms solution. r_1 is the molar longitudinal relaxation rate of water protons in the presence of Fe(III)−C3Ms.

This means that the contrast and the mass of the scattering objects hardly changes. Also dynamic light scattering did not show any changes in hydrodynamic radius, probably because this is determined mainly by the large corona. We tried depolarized dynamic light scattering[27] to check the elongated structure at pH 5, but unfortunately, no significant depolarization signal could be detected due to the small aspect ratio L/d.

Effect of pH on NMR Relaxivity of Fe(III)−C3Ms. A potential application of the Fe(III)−C3Ms studied in this work is as MRI contrast agents. It is therefore important to investigate how the relaxivity depends on the pH. The relaxivity r_1 (molar longitudinal relaxation rate) of Fe(III)−C3M solutions is shown as a function of pH in Figure 7. We find that the relaxivity r_1 is low (1−2.5 mM^{-1} s^{-1}), which is in the same range as that of Fe−EDTA complexes reported by Bloch et al.[28] The relaxivity decreases almost linearly with increasing pH. Above pH 8, the relaxivity of the micellar solution is almost the same as that of pure water. The low relaxivity is due to the strong binding between the ligand and Fe^{3+} ions, which induces a strong crystal field around the metal ions and forces them into a low spin state.[20,29,30] The strong effect of pH must be due to the binding of hydroxide ions.[31] This is quite surprising, as the absorbance spectrum shows that the FeL_2^- complex is the dominating species at pH < 6, suggesting that iron hydroxides do not yet form. A similar decrease of r_1 with pH was also observed for Fe(III)−EDTA complexes.[28] It was argued that the iron in this complex is seven-coordinated, with a water molecule occupying the seventh coordination site. Deprotonation of this coordinated water molecule leads to a strongly reduced proton exchange rate and thereby to a lower relaxivity. Moreover, dinuclear iron(III) complexes can be formed at high pH that are diamagnetic and have almost no effect on proton relaxation.[32] Similar mechanisms could explain the decrease of the relaxivity observed for the Fe(III)−L_2EO_4 complexes studied here. Such a pH-dependent iron coordination is also suggested by the changes observed in the core structure of the micelles.

CONCLUSION

The effect of pH on Fe(III)−C3Ms has been studied by UV/vis spectroscopy, light scattering, Cryo-TEM, and magnetic relaxation measurements. The core of the micelles consists of a coacervate of the anionic iron coordination polymer and a cationic polyelectrolyte block, which is stabilized by a neutral corona. The Fe(III)−L_2EO_4 complexes in the micellar core form striped structures. The coordination polymer in the micellar core is stable in a broad pH range, from 2 to 7. However, the coordination of the metal does change with pH, as observed from a decrease of the proton relaxivity and changes in the internal structure and the shape of the core, which changes from spherical shape (pH 4) to elongated shape (pH 5−7) to a mixture of elongated and branched structures (pH 8). Probably, mixed complexes are formed, in which the iron is coordinated to both the ligand groups and hydroxide ions.

AUTHOR INFORMATION

Corresponding Author

*E-mail: junyou.wang@wur.nl, yunyan@pku.edu.cn.

ACKNOWLEDGMENT

The authors thank Remco Fokkink for help with the light-scattering technique and J. Reedijk for helpful comments. Y.Y. acknowledges financial support from National Nature Science Foundation of China (NSFC, Grant No. 20903005) and the Scientific Research Foundation for the Returned Overseas Chinese Scholars, State Education Ministry (SRF for ROCS, SEM)

REFERENCES

(1) Harada, A.; Kataoka, K. *Science* **1999**, *283*, 65–67.
(2) Kabanov, A. V.; Bronich, T. K.; Kabanov, V. A.; Yu, K.; Eisenberg, A. *J. Am. Chem. Soc.* **1998**, *120*, 9941–9942.
(3) van der Burgh, S.; de Keizer, A.; Cohen Stuart, M. A. *Langmuir* **2004**, *20*, 1073–1084.
(4) Kabanov, A. V.; Bronich, T. K.; Kabanov, V. A.; Yu, K.; Eisenberg, A. *Macromolecules* **1996**, *29*, 6797–6802.
(5) Voets, I. K.; de Keizer, A.; de Waard, P.; Frederik, P. M.; Bomans, P. H. H.; Schmalz, H.; Walther, A.; King, S. M.; Leermakers, F. A. M.; Cohen Stuart, M. A. *Angew. Chem., Int. Ed.* **2006**, *45*, 6673–6676.
(6) Voets, I. K.; de Keizer, A.; Cohen Stuart, M. A.; de Waard, P. *Macromolecules* **2006**, *39*, 5952–5955.
(7) Yan, Y.; Besseling, N. A. M.; de Keizer, A.; Marcelis, A. T. M.; Drechsler, M.; Cohen Stuart, M. A. *Angew. Chem., Int. Ed.* **2007**, *46*, 1807–1809.
(8) Yan, Y.; Besseling, N. A. M.; de Keizer, A.; Cohen Stuart, M. A. *J. Phys. Chem. B* **2007**, *111*, 5811–5818.
(9) Wang, J. Y.; de Keizer, A.; Fokkink, R.; Yan, Y.; Cohen Stuart, M. A.; van der Gucht, J. *J. Phys. Chem. B* **2010**, *114*, 8313–8319.
(10) Vermonden, T.; van der Gucht, J.; de Waard, P.; Marcelis, A. T. M.; Besseling, N. A. M.; Sudholter, E. J. R.; Fleer, G. J.; Cohen Stuart, M. A. *Macromolecules* **2003**, *36*, 7035–7044.
(11) Kabanov, A. V.; Bronich, T. K.; Kabanov, V. A.; Yu, K.; Eisenberg, A. *Macromolecules* **1996**, *29*, 6797–6802.
(12) Solomatin, S. V.; Bronich, T. K.; Bargar, T. W.; Eisenberg, A.; Kabanov, V. A.; Kabanov, A. V. *Langmuir* **2003**, *19*, 8069–8076.
(13) Gohy, J. F.; Varshney, S. K.; Antoun, S.; Jerome, R. *Macromolecules* **2000**, *33*, 9298–9305.
(14) Yuan, X. F.; Harada, A.; Yamasaki, Y.; Kataoka, K. *Langmuir* **2005**, *21*, 2668–2674.
(15) Gohy, J. F.; Varshney, S. K.; Jerome, R. *Macromolecules* **2001**, *34*, 3361–3366.
(16) Yan, Y.; de Keizer, A.; Cohen Stuart, M. A.; Drechsler, M.; Besseling, N. A. M. *J. Phys. Chem. B* **2008**, *112*, 10908–10914.
(17) Biesalski, M.; Johannsmann, D.; Ruhe, J. *J. Chem. Phys.* **2004**, *120*, 8807–8814.
(18) Vermonden, T.; Branowska, D.; Marcelis, A. T. M.; Sudholter, E. J. R. *Tetrahedron* **2003**, *59*, 5039–5045.
(19) Anderegg, G. *Helv. Chim. Acta* **1960**, *43*, 1530–1545.

(20) Bombi, G. G.; Aikebaier, R.; Dean, A.; Marco, V. B. D.; Marton, D.; Tapparo, A. *Polyhedron* **2009**, *28*, 327–335.
(21) Yan, Y.; Lan, Y.; de Keizer, A.; Drechsler, M.; Van As, H.; Cohen Stuart, M. A.; Besseling, N. A. M. *Soft Matter* **2010**, *6*, 3244–3248.
(22) Ding, Y.; Fu, Z. B.; Hu, X. L.; Xia, C. F. *J. Inorg. Organomet. Polym.* **2010**, *20*, 642–648.
(23) Schwarz, G.; Bodenthin, Y.; Geue, T.; Koetz, J.; Kurth, D. G. *Macromolecules* **2010**, *43*, 494–500.
(24) Meister, A.; Forster, G.; Thunemann, A. F.; Kurth, D. G. *ChemPhysChem* **2003**, *43*, 1095–1100.
(25) Haas, W.; Zrinyi, M.; Kilian, H. G.; Heise, B. *Colloid Polym. Sci.* **1993**, *4*, 1024–1034.
(26) Brunner, R.; Gall, S.; Wilke, W.; Zrinyi, M. *Physica A* **1995**, *214*, 153–161.
(27) Lehner, D.; Lindner, H.; Glatter, O. *Langmuir* **2000**, *16*, 1689–1695.
(28) Bloch, J.; Navon, G. *J. Inorg. Nucl. Chem.* **1979**, *42*, 693–699.
(29) Bodenthin, Y.; Pietsch, U.; Mohwald, H.; Kurth, D. G. *J. Am. Chem. Soc.* **2005**, *127*, 3110–3114.
(30) Bodenthin, Y.; Schwarz, G.; Tomkowicz, Z.; Geue, T.; Haase, W.; Pietsch, U.; Kurth, D. G. *J. Am. Chem. Soc.* **2009**, *131*, 2934–2941.
(31) Koenig, S. H.; Baglin, C. M.; Brown, R. D., III *Magn. Reson. Med.* **1985**, *2*, 283–288.
(32) Schugar, H. J.; Rossman, G. R.; Barraclough, C. G.; Gray, H. B. *J. Am. Chem. Soc.* **1972**, *94*, 2683–2690.